4 The Software Package ASICS

Some two years ago I had several small program units with implementations of the theory for analysis of SC NMR spectra described in the previous chapter. However, I discovered that most of the analysis is, in fact, a matter of book-keeping of all the resonances, their rotation angle, -axis, spin transition, etc. Thus, when using several programs that are not completely compatible one has to rewrite the in- and output files to contain the relevant information on all the resonances (in some cases several thousands (*93*, *94*)). Therefore, an obvious thing to do was to make one program which would take care of *all* steps in the analysis.

The software package ASICS – Analysis of Single-Crystal Spectra provides a graphical user-interface[1] to facilitate the interpretation of SC NMR spectra. The analysis is divided into four steps:

1. Measurement of resonance frequencies in the experimental spectra.
2. Assignment of resonances for different rotation angles to different sites/spin transitions in order to generate rotation plots.
3. Correlation of the rotation plots for the three rotation axes for determination of an initial set of parameters.
4. Optimization of the initial parameters and determination of error limits.

With ASICS the SC NMR spectra may be interpreted in terms of the quadrupole coupling and CSA, either one of them or in combination. However, the hetero- and

[1] ASICS requires an X-Windows based workstation, PC with Linux, or an X-Terminal for remote excecution. The software has so far been successfully tested on SUN and Silicon Graphics workstations, and on PC's running Linux.

homo-nuclear dipole coupling interactions will also be implemented in the near future. The input for ASICS is the experimental SC NMR spectra which are stored by ASICS in its own file format.

This chapter focuses on the theory and implementation techniques used, whereas I will refer to the User Guide (appendix B) for an overall view of the features of ASICS. Since it is very tedious to read a manual for a piece of software – especially if you have no access to the program yourself – I do not expect readers of this thesis to carefully read the User Guide. However, it is recommended to spend five minutes skimming through appendix B before reading this chapter.

4.1 Measurement of Resonances in Experimental Spectra

ASICS has an option for interactive and precise deconvolution of the experimental spectra. The reason for having created this feature is that Varian's VNMR software indeed provides commands for deconvolution but - in my opinion - not in a very userfriendly manner. The deconvolution routine in ASICS allows a region of the spectrum to be deconvoluted interactively into one or two resonances, with either Lorentzian or Gaussian lineshape. This action is effectuated by a click on the mouse button and lasts between 0.1 and 2 s.[2] It is possible to fix some of the optimized parameters or include other parameters in the deconvolution. The parameters defining the shape ($\mathcal{S}(\nu)$) of the line are the resonance frequency, $\nu_{\rm res}$, the HHFW linewidth ($\nu_{1/2}$), the intensity ($I_{\rm max}$), the phase (ϕ), and the Gaussian/Lorentzian fraction (Γ). The expression for the lineshape is

$$\begin{aligned} \mathcal{S}(\nu) &= \Gamma \cdot \mathcal{G}(\nu) + (1-\Gamma) \cdot \mathcal{L}(\nu) \\ &= \Gamma \cdot [\mathcal{G}_{\rm r}(\nu)\cos\phi + \mathcal{G}_{\rm i}(\nu)\sin\phi] + (1-\Gamma) \cdot [\mathcal{L}_{\rm r}(\nu)\cos\phi + \mathcal{L}_{\rm i}(\nu)\sin\phi] \end{aligned} \tag{4.1}$$

where $\mathcal{G}(\nu)$ and $\mathcal{L}(\nu)$ represent the Gaussian and Lorentzian lineshapes and the indices r and i refer to the real and imaginary parts of the line. These lineshapes

[2] On a Pentium 150 MHz/Linux 2.0 laptop.

are given by

$$\mathcal{G}_{\mathrm{r}}(\nu^{\star}) = I_{\max} \exp\left\{-\ln 2(\nu^{\star})^2\right\} \tag{4.2}$$

$$\mathcal{G}_{\mathrm{i}}(\nu^{\star}) = I_{\max} \exp\left\{-\ln 2(\nu^{\star})^2\right\} \times \mathrm{erf_i}\left\{\sqrt{\ln 2}\,\nu^{\star}\right\} \tag{4.3}$$

$$\mathcal{L}_{\mathrm{r}}(\nu) = \frac{I_{\max}}{1+(\nu^{\star})^2} \tag{4.4}$$

$$\mathcal{L}_{\mathrm{i}}(\nu) = \frac{I_{\max}\nu^{\star}}{1+(\nu^{\star})^2} \tag{4.5}$$

where $\nu^{\star}$ has been introduced for simplicity ($\nu^{\star} = 2(\nu - \nu_{\mathrm{res}})/\nu_{1/2}$), and $\mathrm{erf_i}$ is the imaginary error function ($\mathrm{erf_i}\{x\} = -i \cdot \mathrm{erf}\{ix\}$) given by the infinite series $\mathrm{erf_i}\{x\} = 2/\sqrt{\pi}\sum_{j=0}^{\infty} 1/j! \cdot x^{2j+1}/(2j+1)$ (*95*).

If the deconvolution involves only one resonance, the initial parameters (ν_{res}, $\nu_{1/2}$, and $I_{\max}$) are determined by fitting the experimental points to a second-order polynomial ($\mathcal{S}_{\mathrm{init}}(\nu) = A\nu^2 + B\nu + C$) and followed by an optimization starting with the initial parameters $\nu_{\mathrm{res}} = -B/2A$, $\nu_{1/2} = \sqrt{D/2A^2}$, and $I_{\max} = -D/4A$ ($D = B^2 - 4AC$) to define the initial lineshape ($\mathcal{S}(\nu)$). The optimization seeks the minimum *rms* deviation between the experimental spectrum and $\mathcal{S}(\nu)$ using Simplex or Powell minimation schemes (*96*). If there are two resonances involved, the initial parameters are defined by the user who uses the mouse to indicate the location of the two resonances. In this case the initial value for $I_{\max}$ is the maximum intensity in the selected region of the spectrum and $\nu_{1/2}$ is the shortest distance from ν_{res} to the upper/lower limit of the selected region of the spectrum.

4.2 Assignment of Resonances

According to the theory the resonances from different rotation angles should be assigned to curves given by

$$\nu^{\mathrm{calc}}(\theta) = A + B\cos 2\theta + C\sin 2\theta \quad (+D\cos 4\theta + E\sin 4\theta) \tag{4.6}$$

for the three-axis goniometer design and

$$\begin{aligned}\nu^{\mathrm{calc}}(\theta) &= A + B\cos\theta + C\sin\theta + D\cos 2\theta + E\sin 2\theta \\ &\quad (+F\cos 3\theta + G\sin 3\theta + H\cos 4\theta + \sin 4\theta)\end{aligned} \tag{4.7}$$

for the two-axis goniometer design. The last terms are in parantheses because they are only relevant for second-order ($\mathcal{H}_\lambda^{(2)}$) interactions.

ASICS helps the assignment by drawing a curve corresponding to the optimum coefficients (A, B, etc.) as soon as a sufficient number of resonances $N_{\min}$ have been assigned manually ($N_{\min} = 3$ for $\mathcal{H}_\lambda^{(1)}$ for the three-axis goniometer, 5 for $\mathcal{H}_\lambda^{(2)}$ (three-axis goniometer) and for $\mathcal{H}_\lambda^{(1)}$ (two-axis goniometer), and $N_{\min} = 9$ for $\mathcal{H}_\lambda^{(2)}$ for the two-axis goniometer). This curve greatly facilitates the further assignment because it indicates which resonances belong to this curve. Whenever a new resonance is selected or deselected, ASICS promptly calculates the new optimized coefficients and draws the line.

The coefficients are determined by minimizing the rms deviation between the experimental, ν_i^{exp}, and calculated, $\nu_i^{\mathrm{calc}} = \nu^{\mathrm{calc}}(\theta_i)$, resonance frequencies:

$$rms = \sqrt{\frac{1}{N}\sum_{i=1}^{N}(\nu_i^{\mathrm{exp}} - \nu_i^{\mathrm{calc}})^2}. \tag{4.8}$$

The minimum rms value is obtained for the values of A, B, etc., where $\partial rms/\partial A = 0$, $\partial rms/\partial B = 0$, etc. The partial derivatives are given by ($\mathcal{H}_\lambda^{(1)}$, three-axis goniometer)

$$\begin{aligned}\frac{\partial rms}{\partial A} &= \frac{1}{N \times rms}\left\{\sum_{i=1}^{N}\left(\nu_i^{\mathrm{exp}} - (A + B\cos 2\theta_i + C\sin 2\theta_i)\right)\right\} \\ &\propto \sum \nu_i^{\mathrm{exp}} - \left(A \times N + B\sum c_i + C\sum s_i\right) \qquad (4.9) \\ \frac{\partial rms}{\partial B} &= \frac{1}{N \times rms}\left\{\sum_{i=1}^{N}\left(\nu_i^{\mathrm{exp}} - (A + B\cos 2\theta_i + C\sin 2\theta_i)\right)\cos 2\theta_i\right\} \\ &\propto \sum \nu_i^{\mathrm{exp}} c_i - \left(A\sum \cos 2\theta_i + B\sum c_i^2 + C\sum s_i c_i\right) \qquad (4.10)\end{aligned}$$

$$\frac{\partial rms}{\partial C} = \frac{1}{N \times rms}\left\{\sum_{i=1}^{N}\left(\nu_i^{\exp} - (A + B\cos 2\theta_i + C\sin 2\theta_i)\right)\cos 2\theta_i\right\}$$
$$\propto \sum \nu_i^{\exp} s_i - \left(A\sum s_i + B\sum c_i s_i + C\sum s_i^2\right) \qquad (4.11)$$

where the short notations c_i and s_i represent $\cos 2\theta_i$ and $\sin 2\theta_i$, respectively. Solving this set of equations for the partial derivatives equal zero corresponds to solving the matrix equation

$$\begin{pmatrix} \sum \nu_i^{\exp} \\ \sum \nu_i^{\exp} c_i \\ \sum \nu_i^{\exp} s_i \end{pmatrix} = \begin{pmatrix} N & \sum c_i & \sum s_i \\ \sum c_i & \sum c_i^2 & \sum c_i s_i \\ \sum s_i & \sum c_i s_i & \sum s_i^2 \end{pmatrix} \times \begin{pmatrix} A \\ B \\ C \end{pmatrix} \qquad (4.12)$$

which is easily handled by a computer (*97*).[3] It is noted that when $N \geq N_{\min}$ this is normally a non-singular set of equations, i.e., it has only one solution vector.

4.2.1 Semi-Automatic Assignment

Although I have tried to make a fully automatic assignment algorithm, it turns out that such an algorithm needs too many inputs to be efficient. For example, we may visually recognize some curves in the rotation plots and we know whether a curve originates from a first- or second-order interaction. Such informations are difficult to feed into a computer in a simple manner. Therefore, I have attempted to make an algorithm for semi-automatic assignment of the resonances. That is, when the first $N_{\min}$ resonances have been assigned, the computer may be ordered to perform the remaining assignment of this particular line.

Figure 4.1a illustrates the problem we are facing. It shows a rotation plot ($\mathcal{H}_{\mathrm{Q}}^{(2)}$, three-axis goniometer) with five resonances assigned and marked with large circles. The curve represents the optimum coefficients. From this rotation plot it is obvious that the further assignment should start from the group of resonances

[3]Even for the nine-dimensional matrix that results from $\mathcal{H}_{\lambda}^{(2)}$ for the two-axis goniometer design, the coefficients are determined in less than 1 ms on a Pentium 150 MHz/Linux 2.0 laptop.

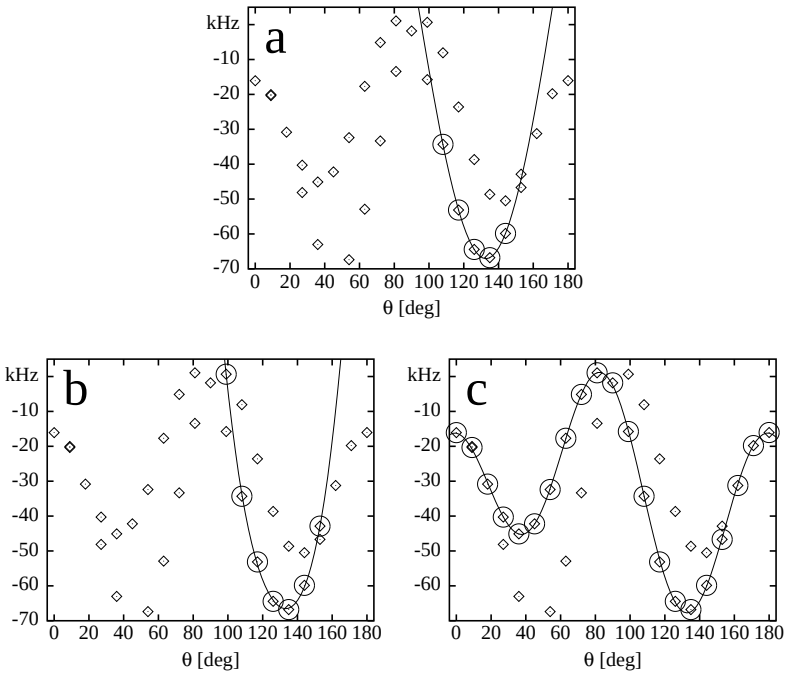

Figure 4.1: Illustration of the problems encountered in a semi-automatic assignment procedure. (a) Five resonances are manually assigned (marked with large circles). (b) The assignment obtained by a procedure that starts the assignments from the group of assigned resonances. (c) Result of the two-step assignment procedure described in the text. In this case all resonances are correctly assigned.

already assigned and not just from one end ($\theta = 0°$ or $180°$). The assignment starts with the near neighbours to the group of assigned resonances, e.g., with the rotation angle $\theta = 108°$ or $153°$ and assign a resonance provided it is located within a predefined interval ($\Delta\nu$) away from this calculated resonance frequency. In the present case the two resonances at $\theta = 153°$ are both within the interval $\nu^{\mathrm{calc}} \pm \Delta\nu$. Unfortunately the wrong resonance is closer to ν^{calc} at this stage, resulting in an uncorrect assignment as shown in fig. 4.1b.

A more stable algorithm relies on a two-step assignment procedure. In first "scan" through the rotation angles a resonance is assigned provided they are within the range $\Delta\nu$ from the calculated resonance frequency and *provided it is the only resonance within the interval* $\nu^{\mathrm{calc}} \pm \Delta\nu$ *for this rotation angle.* In the second "scan" any resonance that is within this interval is assigned, however, if there are two or more resonances within this range for the same rotation angle, the resonance being

the shorter distance from ν^{calc} is selected. The resulting assignment in the present example is shown in fig. 4.1c, and we observe that using this algorithm all the resonances are correctly assigned.

4.3 Correlation Between the Three (Two) Rotation Axes

For correlation of the curves from the different rotation axes it is useful to recall that some spectra for the different rotation axes are identical since they only differ by rotation about the direction of the magnetic field (eqs. 2.1 - 2.5 on page 22). These identities are important as they provide a way to do the correlation. On the basis of the optimum coefficients for the different rotation axes ASICS calculates the expected resonance frequency for the relevant rotation angles in eqs. 2.1 - 2.3 or 2.4 - 2.5 for each curve. Thus it is usually a straight-forward matter to perform the correlation.

4.3.1 Determination of Preliminary Parameters

Having performed the correlation it is possible to determine a preliminary set of parameters for the desired interaction(s) by use of the coefficients for the different rotation axes. The procedure is to determine the tensors $\boldsymbol{\lambda}^{\mathrm{T}}$ from the expressions for the coefficients listed in tables 3.3 and 3.4 and subsequently diagonalize these tensors to obtain the interaction parameters.

As mentioned in the introduction, SC NMR gives a unique possibility for separation of the quadrupole coupling and CSA interactions. For the satellite transitions we may use that the quadrupole coupling interaction is proportional to I_z^2 while the CSA interaction is proportonal to I_z. Therefore the splitting between symmetric satellite transitions ($\nu_{m\leftrightarrow m-1} - \nu_{-m\leftrightarrow -m+1}$) will only be influenced by $\mathcal{H}_{\mathrm{Q}}^{(1)}$ while the CSA terms disappear. On the other hand, the sum of two symmetric satellite transitions will only be influenced by the CSA. For the central transition of half-integer

quadrupolar nuclei the $\cos n\theta$ and $\sin n\theta$ terms with $n > 2$ in the equation for the rotational dependence of the resonance frequency (eq. 4.6 or 4.7) are unique to the quadrupole coupling interaction. Thus, it is possible to determine the quadrupole coupling tensor from the coefficients for these terms and then afterwards determine the CSA tensor from the remaining terms.

The quadrupole coupling tensor is traceless whereas the trace of the shielding tensor is proportional to the isotropic chemical shift. In many cases δ_{iso} is much larger than δ_σ which may introduce inaccuracies in numerical manipulations of the CSA tensor. Because the isotropic chemical shift just corresponds to a constant frequency shift, ASICS operates with a traceless shielding tensor (i.e., $\mathrm{Tr}\{\mathbf{Q}\} = \mathrm{Tr}\{\boldsymbol{\sigma}\} = 0$) and corrects for the isotropic chemical shift afterwards.

The First-Order Interactions

From the expressions for the first-order coefficients, $M^{\lambda,1}_{m,\alpha}$, for the three-axis goniometer (table 3.3) the $\lambda^{\mathrm{T}}_{\alpha\beta}$ tensor elements may be isolated according to

$$\lambda^{\mathrm{T}}_{xy} = C^{\lambda,1}_{m,z} k^\lambda_m \tag{4.13}$$

$$\lambda^{\mathrm{T}}_{xz} = -C^{\lambda,1}_{m,y} k^\lambda_m \tag{4.14}$$

$$\lambda^{\mathrm{T}}_{yz} = -C^{\lambda,1}_{m,x} k^\lambda_m \tag{4.15}$$

$$\begin{aligned}\lambda^{\mathrm{T}}_{xx} &= \left(A^{\lambda,1}_{m,y} - B^{\lambda,1}_{m,y} - \frac{1}{3}\left[A^{\lambda,1}_{m,x} + A^{\lambda,1}_{m,y} + A^{\lambda,1}_{m,z}\right]\right) k^\lambda_m \\ &= \left(A^{\lambda,1}_{m,z} + B^{\lambda,1}_{m,z} - \frac{1}{3}\left[A^{\lambda,1}_{m,x} + A^{\lambda,1}_{m,y} + A^{\lambda,1}_{m,z}\right]\right) k^\lambda_m \end{aligned} \tag{4.16}$$

$$\begin{aligned}\lambda^{\mathrm{T}}_{yy} &= \left(A^{\lambda,1}_{m,x} - B^{\lambda,1}_{m,x} - \frac{1}{3}\left[A^{\lambda,1}_{m,x} + A^{\lambda,1}_{m,y} + A^{\lambda,1}_{m,z}\right]\right) k^\lambda_m \\ &= \left(A^{\lambda,1}_{m,z} - B^{\lambda,1}_{m,z} - \frac{1}{3}\left[A^{\lambda,1}_{m,x} + A^{\lambda,1}_{m,y} + A^{\lambda,1}_{m,z}\right]\right) k^\lambda_m \end{aligned} \tag{4.17}$$

$$\begin{aligned}\lambda^{\mathrm{T}}_{zz} &= \left(A^{\lambda,1}_{m,x} + B^{\lambda,1}_{m,x} - \frac{1}{3}\left[A^{\lambda,1}_{m,x} + A^{\lambda,1}_{m,y} + A^{\lambda,1}_{m,z}\right]\right) k^\lambda_m \\ &= \left(A^{\lambda,1}_{m,y} + B^{\lambda,1}_{m,y} - \frac{1}{3}\left[A^{\lambda,1}_{m,x} + A^{\lambda,1}_{m,y} + A^{\lambda,1}_{m,z}\right]\right) k^\lambda_m \end{aligned} \tag{4.18}$$

where $k_m^{\mathrm{Q}} = 1/(3[m-1/2])$ and $k_m^{\sigma} = 1/\nu_0$. The tensor $(\boldsymbol{\lambda}^{\mathrm{T}})$ is traceless and thus we need to determine the isotropic chemical shift also:

$$\delta_{\mathrm{iso}} = \frac{1}{3\nu_0}\left(A_{m,x}^{\lambda,1} + A_{m,y}^{\lambda,1} + A_{m,z}^{\lambda,1}\right). \tag{4.19}$$

For the two-axis goniometer the $\lambda_{\alpha\beta}^{\mathrm{T}}$ tensor elements are given by

$$\lambda_{xy}^{\mathrm{T}} = \frac{C_{m,a}^{\lambda,1} + C_{m,b}^{\lambda,1}}{2\sin\phi}k_m^{\lambda} = \frac{E_{m,a}^{\lambda,1} + E_{m,b}^{\lambda,1}}{\cos\phi}k_m^{\lambda} \tag{4.20}$$

$$\lambda_{xz}^{\mathrm{T}} = \frac{A_{m,b}^{\lambda,1} - A_{m,a}^{\lambda,1}}{\cos\phi\sin\phi}k_m^{\lambda} = \frac{B_{m,a}^{\lambda,1} - B_{m,b}^{\lambda,1}}{2(\cos^2\phi - \sin^2\phi)}k_m^{\lambda} = \frac{D_{m,a}^{\lambda,1} - D_{m,b}^{\lambda,1}}{\cos\phi\sin\phi}k_m^{\lambda} \tag{4.21}$$

$$\lambda_{yz}^{\mathrm{T}} = \frac{C_{m,a}^{\lambda,1} - C_{m,b}^{\lambda,1}}{2\cos\phi}k_m^{\lambda} = \frac{E_{m,a}^{\lambda,1} - E_{m,b}^{\lambda,1}}{\sin\phi}k_m^{\lambda} \tag{4.22}$$

$$\lambda_{xx}^{\mathrm{T}} = \left[(D_{m,a}^{\lambda,1} + D_{m,b}^{\lambda,1}) - (B_{m,a}^{\lambda,1} + B_{m,b}^{\lambda,1})\frac{1+\sin^2\phi}{2\cos\phi\sin\phi}\right]\frac{k_m^{\lambda}}{3} \tag{4.23}$$

$$\lambda_{zz}^{\mathrm{T}} = \frac{B_{m,a}^{\lambda,1} + B_{m,b}^{\lambda,1}}{2\cos\phi\sin\phi}k_m^{\lambda} + \lambda_{xx}^{\mathrm{T}} \tag{4.24}$$

$$\lambda_{yy}^{\mathrm{T}} = -\lambda_{xx}^{\mathrm{T}} - \lambda_{zz}^{\mathrm{T}} \tag{4.25}$$

and the isotropic chemical shift is determined as

$$\delta_{\mathrm{iso}} = \frac{1}{2\nu_0}\left[A_{m,a}^{\lambda,1} + A_{m,b}^{\lambda,1} - \left(\lambda_{yy}^{\mathrm{T}} + \lambda_{xx}^{\mathrm{T}}(1+\sin^2\phi) + \lambda_{zz}^{\mathrm{T}}(1+\cos^2\phi)\right)k_m^{\lambda}\right]. \tag{4.26}$$

In eqs. 4.16-4.18 and 4.20-4.22 there is more than one solution and to minimize the experimental error ASICS uses the average of the different solutions in these cases.

The Second-Order Quadrupole Interaction

For the three-axis goniometer design we may readily determine the quadrupole coupling tensor from the $D_{1/2,\alpha}^{\mathrm{Q},2}$ and $E_{1/2,\alpha}^{\mathrm{Q},2}$ terms because $D_\alpha = D_{1/2,\alpha}^{\mathrm{Q},2}$ and $E_\alpha = E_{1/2,\alpha}^{\mathrm{Q},2}$ where D_α and E_α represent the experimentally determined coefficients. The

$\mathbf{Q}^{\mathrm{T}}$ tensor elements are given by

$$\left(Q^{\mathrm{T}}_{\alpha\alpha} - Q^{\mathrm{T}}_{\beta\beta}\right)^2 = \frac{64\nu_0}{9(4I(I+1)-3)}\left(D^{\mathrm{Q},2}_{1/2,\gamma} + \sqrt{D^{\mathrm{Q},2}_{1/2,\gamma} + E^{\mathrm{Q},2}_{1/2,\gamma}}\right) \quad (4.27)$$

$$\left(Q^{\mathrm{T}}_{\alpha\beta}\right)^2 = \frac{16\nu_0}{9(4I(I+1)-3)}\left(-D^{\mathrm{Q},2}_{1/2,\gamma} + \sqrt{D^{\mathrm{Q},2}_{1/2,\gamma} + E^{\mathrm{Q},2}_{1/2,\gamma}}\right) \quad (4.28)$$

($\alpha, \beta, \gamma = x, y, z$ or a permutation) except from the sign of the quadrupole coupling constant, which is abitrarily chosen to be positive. Since eqs. 4.27 and 4.28 each represents three equations and $\mathrm{Tr}\{\mathbf{Q}\} = 0$ there are seven equations to describe the six tensor elements of the quadrupole coupling tensor. To minimize the effect of the experimental errors ASICS optimizes the quadrupole coupling parameters to the best fit to eqs. 4.27 and 4.28 with the restriction that the quadrupole coupling tensors should be traceless.

Having determined the quadrupole coupling tensor we may readily calculate the coefficients $A^{\mathrm{Q},2}_{1/2,\alpha}$, $B^{\mathrm{Q},2}_{1/2,\alpha}$, and $C^{\mathrm{Q},2}_{1/2,\alpha}$ by use of the expressions in table 3.3, and subsequently calculate the contribution from the CSA as

$$A^{\sigma,1}_{1/2,\alpha} = A_\alpha - A^{\mathrm{Q},2}_{1/2,\alpha} \quad (4.29)$$

etc. and calculate the CSA tensor by use of eqs. 4.13-4.18.

For the two-axis goniometer the four terms F_α, G_α, H_α, and I_α for each rotation axis are only influenced by the quadrupole coupling interaction ($M_\alpha = M^{\mathrm{Q},2}_{1/2,\alpha}$). However, there is no analytical solution to the expressions for these coefficients, and, therefore, the procedure used by ASICS is to optimize the quadrupole coupling parameters to the eight $M^{\mathrm{Q},2}_{1/2,\alpha}$ coefficients by using the initial parameters

$$C_{\mathrm{Q}} = \nu_0 \times 0.152\sqrt[4]{\textstyle\sum_M (M_\alpha)^2}, \quad \eta_{\mathrm{Q}} = 0, \quad \alpha_{\mathrm{Q}} = \beta_{\mathrm{Q}} = \gamma_{\mathrm{Q}} = 0^\circ \quad (4.30)$$

where the expression for C_{Q} is a fairly precise empirically determined relation. This turns out to be a very stable procedure which always returns the correct quadrupole

coupling tensor elements.

The Relative Orientation of the Quadrupole Coupling and CSA Tensors

It is most convenient to express the orientation of the CSA tensor in the P_Q frame rather than in the tenon frame as described in the previous chapter. Thus after diagonalization of the two tensors,

$$\boldsymbol{\lambda}^{\mathrm{T}} = \mathbf{R}_\lambda(\Omega_\lambda)\boldsymbol{\lambda}^{\mathrm{P}}\mathbf{R}_\lambda^T(\Omega_\lambda), \tag{4.31}$$

the relative orientation of the two tensors is determined as

$$\widetilde{\mathbf{R}}_\sigma(\psi,\chi,\xi) = \mathbf{R}_{\mathrm{Q}}^T(\Omega_{\mathrm{Q}})\mathbf{R}_\sigma(\Omega_\sigma). \tag{4.32}$$

and used further on in the analysis.

4.4 Optimization of the Parameters and Calculation of Confidence Intervals

The procedure for determination of the NMR parameters as described in the previous section does not properly take the experimental errors into account. That is, the procedure described assumes that all coefficients are determined with equal precision. Moreover, it is often desirable to fix some parameters (e.g., the crystal symmetry imposes restrictions on some of the parameters) during optimization or to perform a simultaneous optimization of parameters for several spin transitions or crystallographically equivalent but magnetically nonequivalent nuclei. Therefore ASICS gives the possibility for optimization of the parameters according to minimum rms deviation between the experimental and calculated resonance frequencies for all rotation axes and for all the included sites/transitions.

The optimization is performed either by a Simplex or a Powell minimation al-

gorithm (*96*), and all parameters may either be optimized or fixed during the optimization. This also provides the possibility for calculation of confidence intervals. Generally the 95% confidence intervals are used to indicate the error limit for the parameters. However, one should be careful not to rely too much on these error limits because they represent the statistical error and do not include experimental errors. Therefore, by increasing the number of resonances the confidence interval diminishes, but this does not necessarily imply that the "reliable" error limits are diminished correspondingly. However, the confidence intervals always provide a very good measure for the relative precision of the individual parameters.

The confidence interval for a parameter p is determined from the curvature of the $\chi^2(p)$ function

$$\chi^2 = \sum_{i=1}^{N} \left(\frac{\nu_i^{\mathrm{exp}} - \nu_i^{\mathrm{calc}}}{\sigma_i} \right)^2 \qquad (\propto rms^2) \tag{4.33}$$

near the optimum value for p, p_{opt} (σ_i is the measurement error for ν_i^{exp}). According to the theory (*73*) the curvature of the $\chi^2(p)$ function may be approximated to a second-order polynomial: $\chi^2(p) \approx Ap^2 + Bp + C$, and the 95% confidence is given by $\delta_{95\%}(p) = 2/\sqrt{A}$.

ASICS automatically calculates the 95% confidence intervals by fixing the parameter p at different values near its optimum value and for each value of p perform an optimization of all other parameters for determination of $\chi^2(p)$. The small increments for p are predefined according to the knowledge of typical values for the error limits of each parameter. In order to limit the number of optimizations needed ASICS starts at the optimum value for p and steps away from this value towards larger values for p. When $\chi^2(p)$ exceeds $\chi^2(p_{\mathrm{opt}}) + 6$ the 95% confidence limit is reached, and ASICS steps in the other direction (from p_{opt} towards smaller values for p) until the 95% confidence limit is reached. From these data the 95% confidence interval is calculated right away.

The measurement error σ_i may or may not be included. Normally these errors

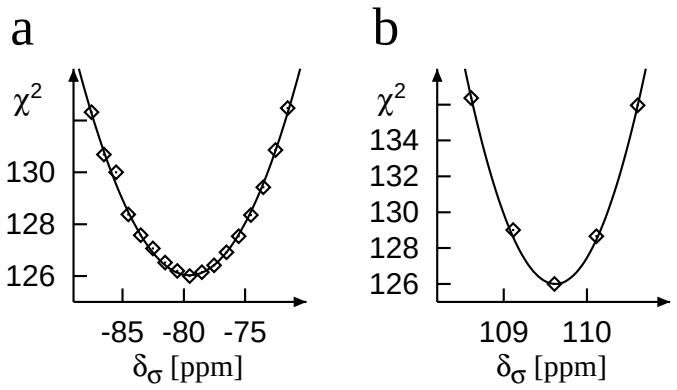

Figure 4.2: χ^2 optimizations of δ_σ for the two Rb sites in Rb_2CrO_4. The experimental points ($\diamond$) correspond to the minimum χ^2 value obtained for different fixed values of δ_σ for Rb sites 1 (a) and 2 (b). The solid lines represent the optimum second-order polynomial which is used to calculate the 95% confidence interval for δ_σ (Rb(1): $\delta_\sigma = -80 \pm 7$ ppm, Rb(2): $\delta_\sigma = -109.7 \pm 0.6$ ppm).

are unknown, and thus ASICS has adopted the suggestion in ref. *73* and uses the value $\sigma_i = rms(p_{\mathrm{opt}})$. However, there are two ways to include the measurement error by (*i*) calculation of 95% confidence interval for the resonance frequencies determined from the convolution of the experimental spectra (this would be very time-consuming) or (*ii*) assume that the measurement error is proportional to the linewidth of the resonances.

For demonstration of the confidence-interval calculation fig. 4.2 shows plots of $\chi^2(p)$ for different fixed δ_σ values for the two Rb sites in Rb_2CrO_4 (see section 5.1.4). This figure clearly shows well-defined minima for χ^2 for both site 1 (a) and 2 (b), and the 95% confidence intervals are calculated from the optimum second-order polynomial shown with solid lines in fig. 4.2.